ANNUAL REPORT 2010

UIUC, August 12, 2010

Analysis of off-corner longitudinal crack formation in slab casting and comparison of hot-tearing criteria

Junya Iwasaki
(Visiting scholar from Nippon Steel)

Department of Mechanical Science and Engineering
University of Illinois at Urbana-Champaign

Objective

- To reconstruct the circumstances of Breakout caused by off-corner crack at Yawata works, using computational model
- To develop hypotheses on longitudinal crack mechanisms at off-corner in slab casting
- To quantify the effect of trilinear profile of narrow face mold currently in use at Yawata works.

Outline

1. The Circumstances of Breakout
2. CON1D Model Fitting Condition
3. Thermal Mechanical Behavior with ABAQUS
4. Evaluation of Hot-tearing Criteria
5. Conclusions

1. The Circumstances of Breakout

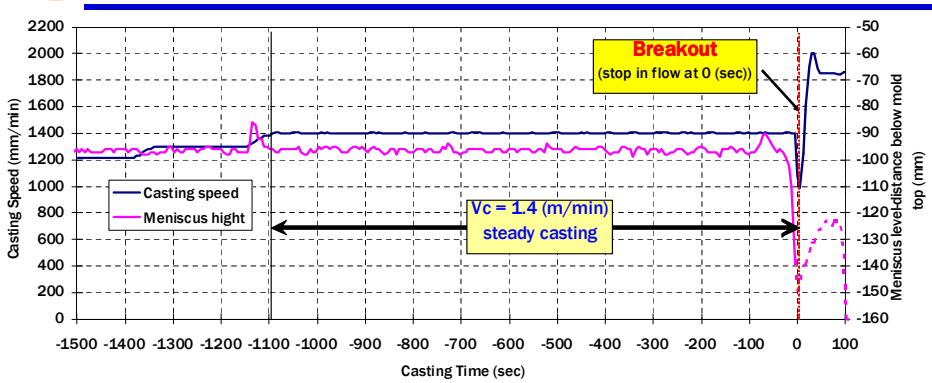

Figure 1. History of recorded Casting Conditions around breakout

Table 1. Casting Condition

		Steel Composition	
Casting speed	23.4 mm/s		
Strand thickness	252 mm	0.16	%C
Strand width	1360 mm	0.71	%Mn
SEN submergence depth	230 mm	0.016	%P
Pour temperature	1540 ℃	0.006	%S
Meniscus dist. From mold top	96 mm	0.02	%Si
Mold conductivity (WF)	242 W/mK	0.039	%Al
(NF)	355 W/mK		

1. The Circumstances of Breakout

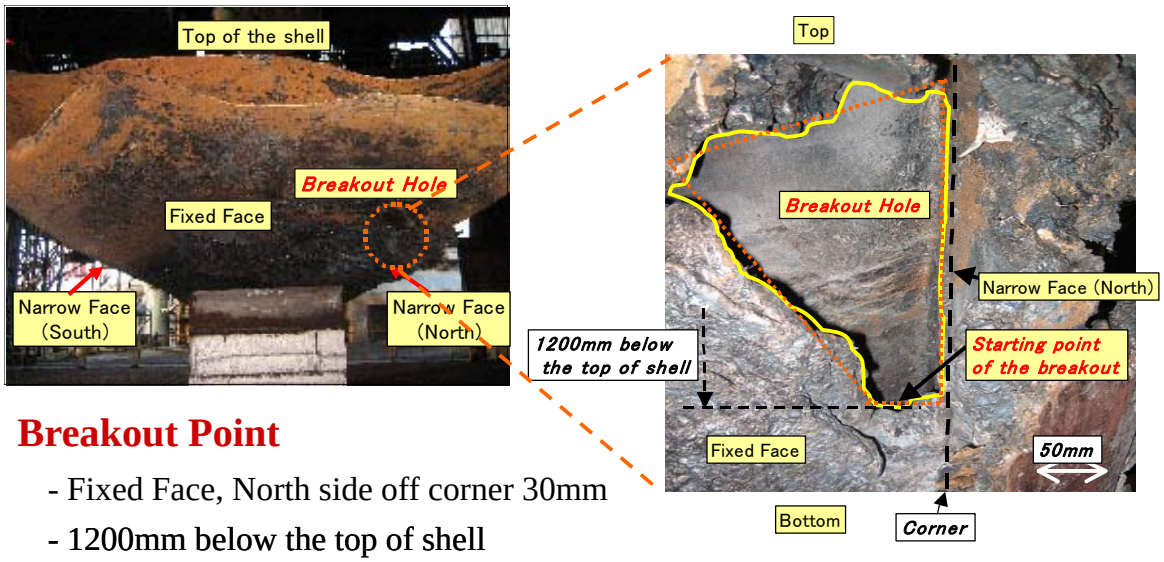

Breakout Point

- Fixed Face, North side off corner 30mm
- 1200mm below the top of shell
- Hole size = 34107 mm^2

Figure 2. Breakout shell and hole

1. The Circumstances of Breakout

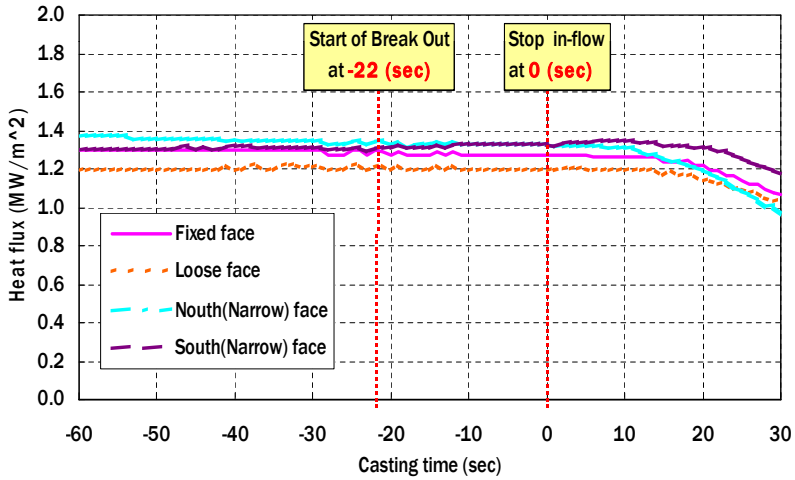

~constant q:

1.279MW/m² (Fixed face)

1.195MW/m2 (Loose face)

1.336MW/m2 (Nouth face)

1.294MW/m2 (South face)

(Average from -1000s to -23s
; Vc = 1.4 m/min ~ constant)

Figure 3. History of recorded Heat Flux during Breakout

2. CON1D Model Fitting conditions of Breakout condition

Table 2. CON1D Fitting Condition

	Fixed face	Narrow face
Simulation shell	Fixed face	
Casting speed	23.4 mm/s	
SEN submergence depth	230 mm	
Pour temperature	1540 ℃	
Meniscus dist. From mold top	96 mm	
Fraction solid for shell thickness location	0.35	
Treatment of superheat	-	1 : default
Mean heat flux in mold - measured	1.279 MW/m^2	1.294 MW/m^2
Fitting Parameters		
- Solid flux conductivity	1.00 W/mK	
- Liquid flux conductivity	1.00 W/mK	
- Location of peak heat flux	-	0.03 m
- Slag rim thickness at metal level	-	2.20 mm
- Slag rim thickness at heat flux peak	-	0.75 mm
- Cold face scale thickness	-	0.002 mm
- Constant ratio of solid flux velocity to casting speek	0.085	0.084
CON1D prediction		
- Mean heat flux in mold	1.279 MW/m^2	1.293 MW/m^2

2.1. Calculated Heat Flux

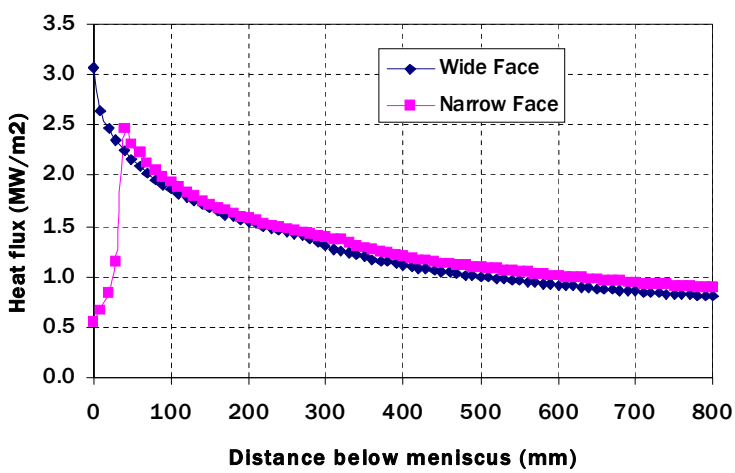

Figure 4. CON1D calculated Heat Flux profile

2.2. Estimated Solidification Time

Note: Eulerian frame of reference (based on steady-meniscus position)

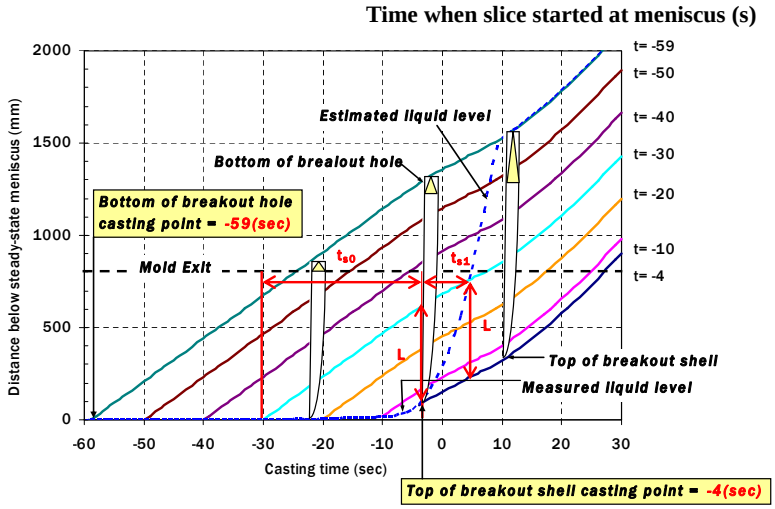

Figure 5. Distance traveled by different points on the shell surface relative to the dropping

$$t_s = t_{s0} + t_{s1} \quad \ldots (1)$$

$$\int_{t_{s0}}^{t_{-4}} V_C dt = L \quad \ldots (2)$$

$$\int_{t_{-4}}^{t_{s1}} \left(\frac{dz}{dt} - V_C\right) dt = L \quad \ldots (3)$$

- t_s : solidification time at L (sec)
- t_{s0} : solidification time at L before -4 (sec)
- t_{s1} : solidification time at L after -4 (sec)
- V_C : casting speed (m/min)
- z : distance below steady state maniscus to liquid level(m)
- L : distance from the top of shell (m)

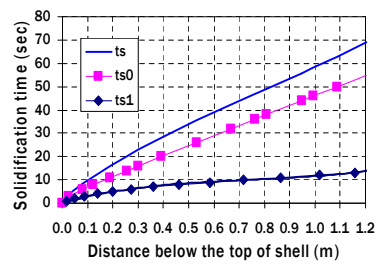

Figure 6. Solidification time

2.3. CON1D Model Verification with Plant

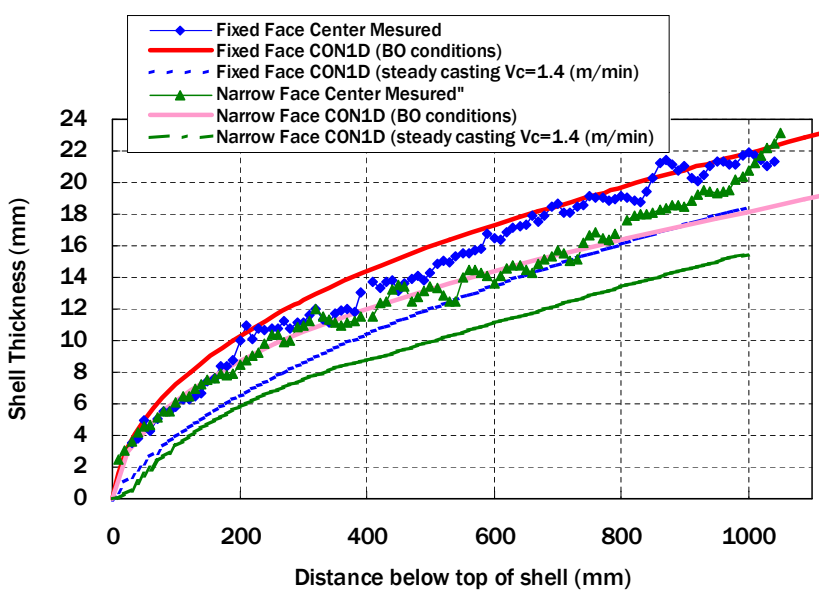

Figure 7. Comparison between CON1D calculated profile and measurements from BO shell

2.3. CON1D Model Verification with Plant

Wide Face

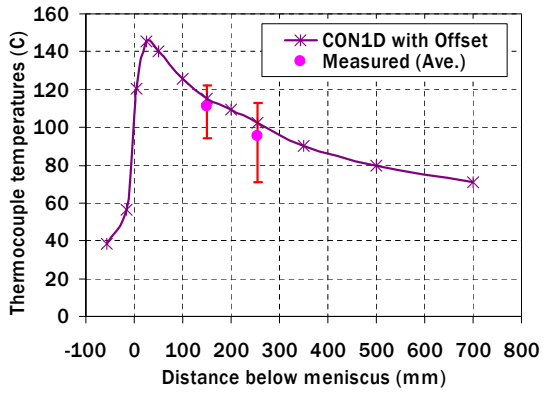

Narrow Face

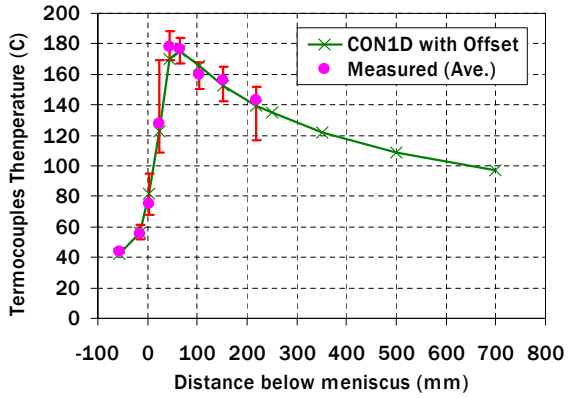

Figure 8. Thermocouple temperatures comparison between CON1D and Measured data

2.4. CON1D calculated Slag layer Thickness

Wide Face

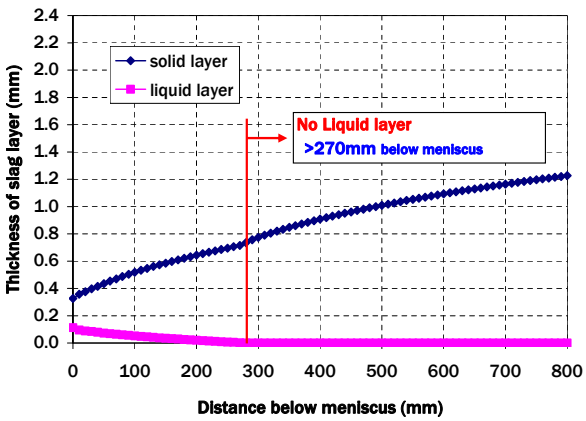

Narrow Face

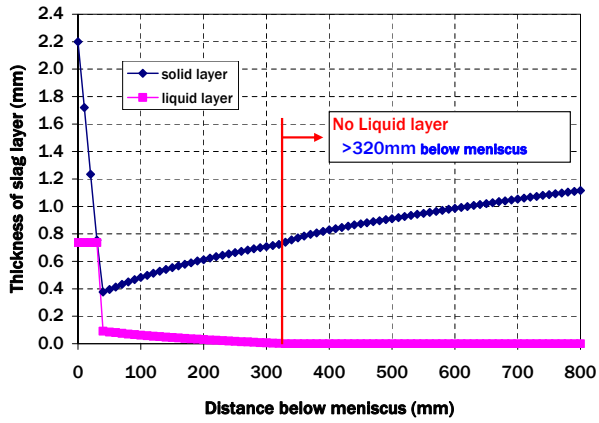

Figure 9. CON1D calculated Slag layer Thickness

3. Thermal-Mechanical Behavior with ABAQUS

3.1. Steel properties

Kagawa and Okamoto, Mat. Sci. and Technology col.2 Oct. 1986 p.997

…same calculation as CON1D subroutine phase1.

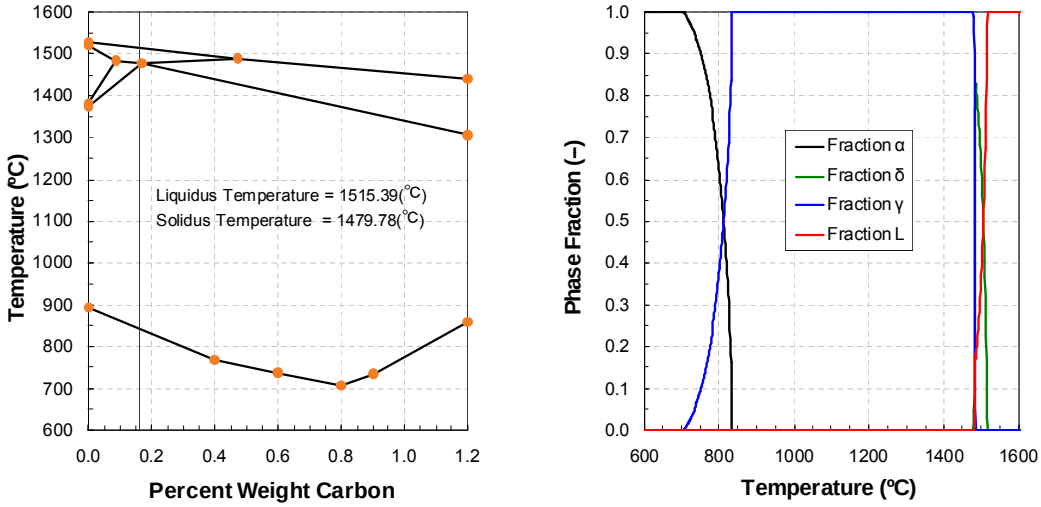

Figure 10. Phase Diagram and Phase Fraction

3.1. Steel properties

Thermal Conductivity

Specific Heat

Coefficient of Thermal Expansion

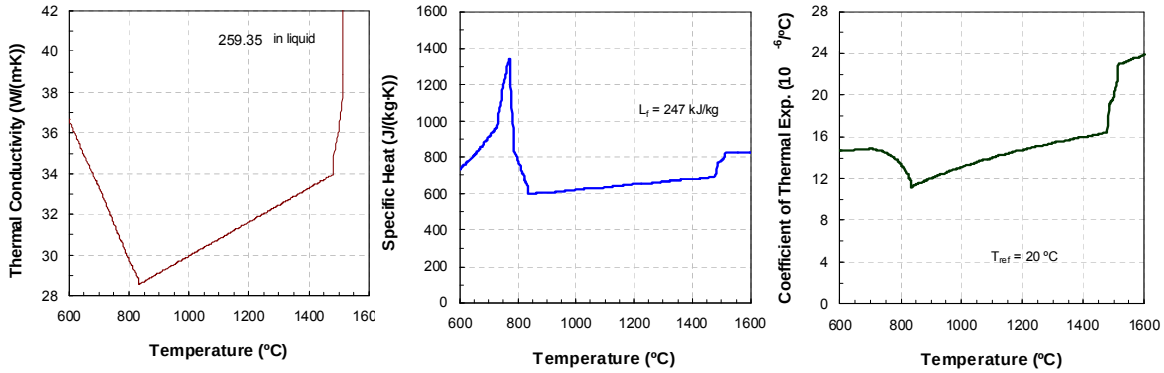

Figure 11. Steel Properties

3.2. Procedure for coupled thermal-stress analysis

Step 1

- Analyze Corner Gap with ABAQUS thermal stress model.

Step 2

- Calculate Heat Flux at corner region for this Corner Gap profile with spread sheet.

Step 3

- Re-analyze Strain behavior using new Heat Flux at corner region with ABAQUS.

3.3. Process Parameter

Table 3. Process Parameter

Casting speed	**1402 mm/min**
Mold length	**900 mm**
Meniscus dist. From mold top	**96 mm**
Time in mold	**34.25 sec**
Slab width at Meniscus	**1360 mm**
Slab thickness at Meniscus	**258 mm**
Narrow face taper	**9.5 mm/side**
	(1.56 %/m)
Carbon content	**0.1617 wt.%**
Solidus temperature	**1479.78 ^{o}C**
Liquidus temperature	**1515.39 ^{o}C**
Pour temperature	**1540 ^{o}C**

3.4. Parametric Study

Table 4. Important Parameters for simulation

	CASE 1	CASE 2	CASE 3	CASE 4	CASE 5	CASE 6	CASE 7
Corner gap contains:	Liquid Flux and Air	Liquid Flux	Air	Liquid Flux and Air			
Mold distortion	No			New Waterbox	Est. Old Waterbox 3.8X larger	No	
Depression	No					Yes	No
Narrow face taper profile	linear						trilinear

3.5. Corner gap schematics: 7 cases

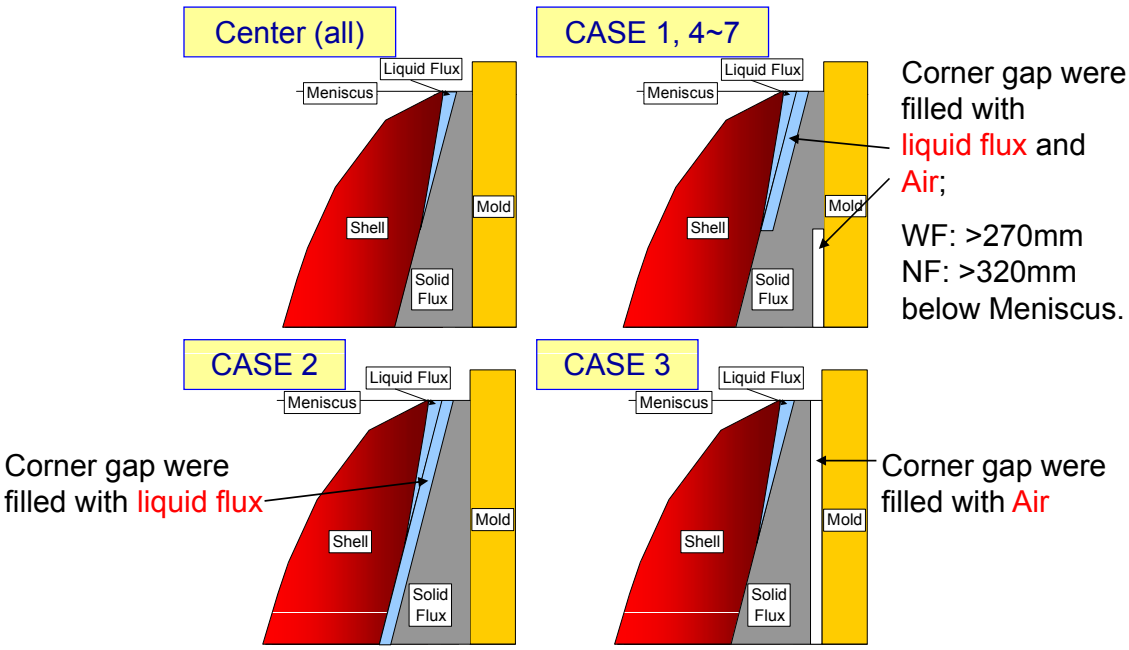

Figure 12. Difference between CASES

3.6. Mold Distortion

Wide face and Narrow face Mold Distortion condition was calculated individually by FEM.

Wide face

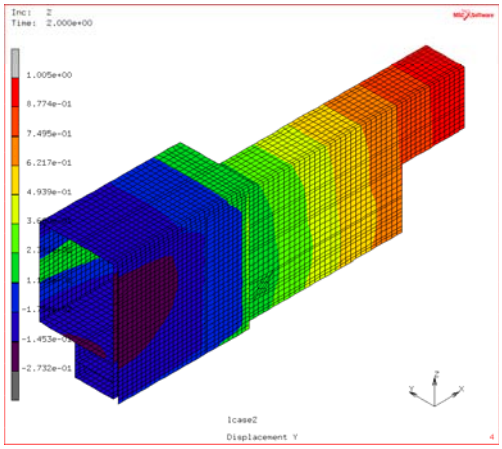

Narrow face

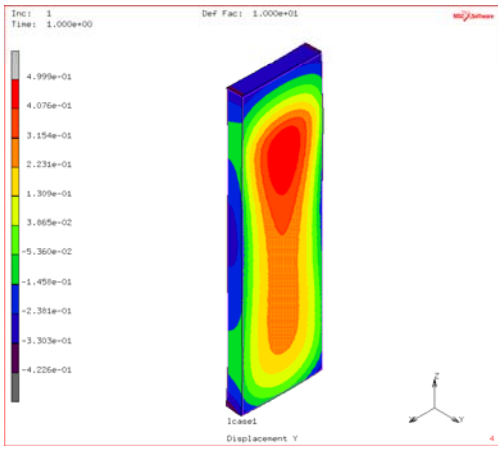

Figure 13. Mold Distortion Analysis

3.7. Mold Distortion

CASE 4

Wide face

+: Shell side

- : Mold side

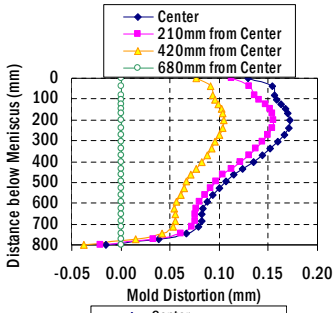

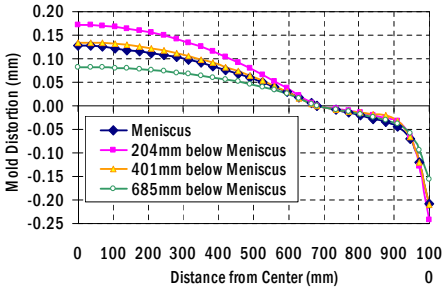

Narrow face

+: Mold side

- : Shell side

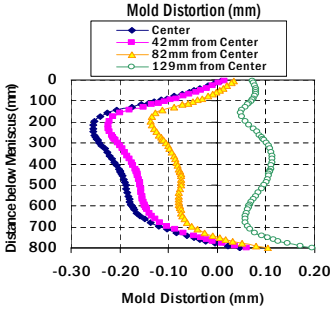

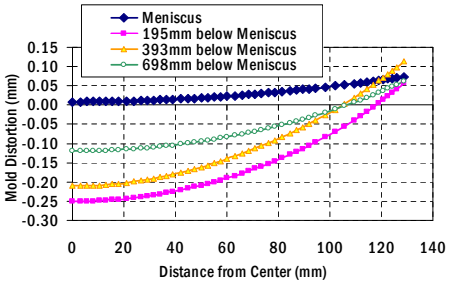

Figure 14. Analyzed Mold Distortion

CASE 5

CASE 5 is 3.8 times bigger than CASE 4.

(compared with polar moment of inertia of area)

3.8. Surface depression at off-corner

Figure 15. Surface depression at off-corner – filled with flux

3.9. Narrow face taper

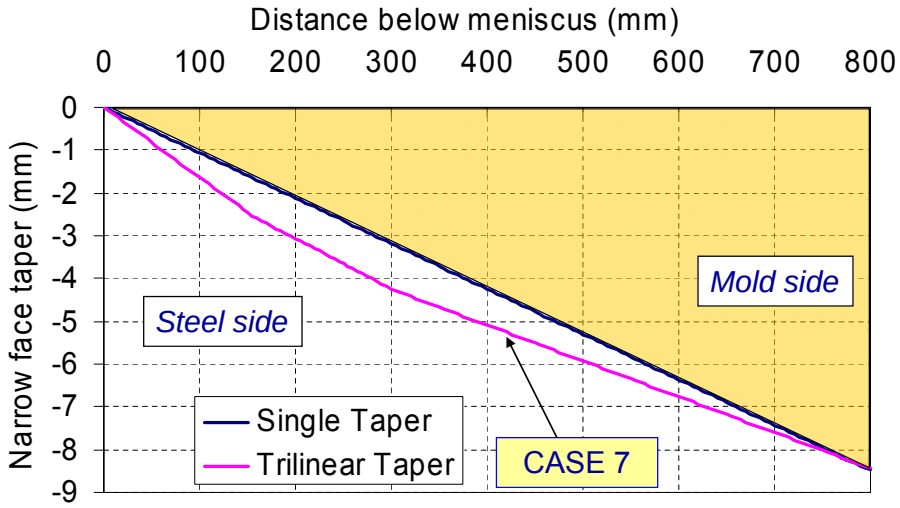

Figure 16. Narrow face taper profile

3.10. Shell-Mold Interfacial Heat Flux - Step 1

Step 1

Wide face

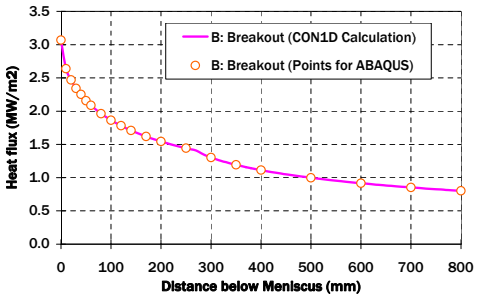

Narrow face

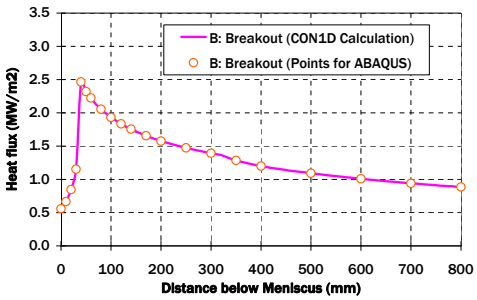

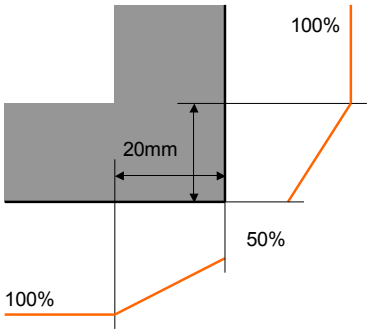

Decrease heat flux at corner to account for gap formation

(linear drop to 50% over 20mm)

Figure 17. Shell-Mold Interfacial Heat Flux at Step 1

3.11. Simulated Shell domain and Mesh

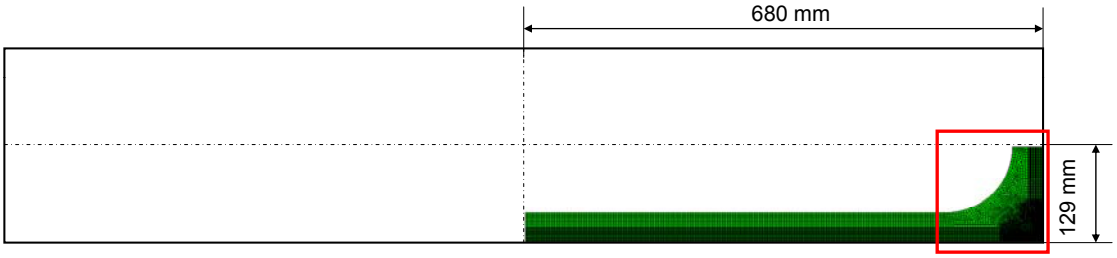

Figure 18. Simulated Shell Domain and Mesh

Number of elements : 33627 (CASE 1,2,3,7)

34385 (CASE 4,5)

33730 (CASE 6)

(quadrilateral and triangular

generalized plane strain, hybrid finite elements)

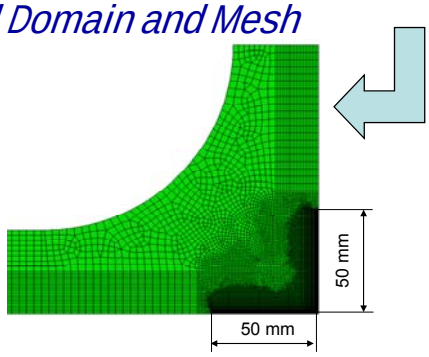

Figure 19. Detail of Corner of Shell Domain

3.12. Analyzed result – Step 1

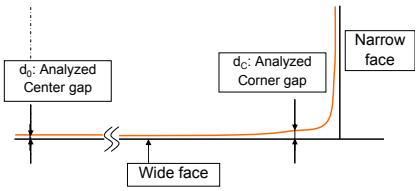

$$d_g = d_C - d_0 \quad \ldots (4)$$

d_g = Corner Gap (mm)
d_0 = Analyzed Center Gap (mm)
d_C = Analyzed Corner Gap (mm)

20x Magnified Displacement

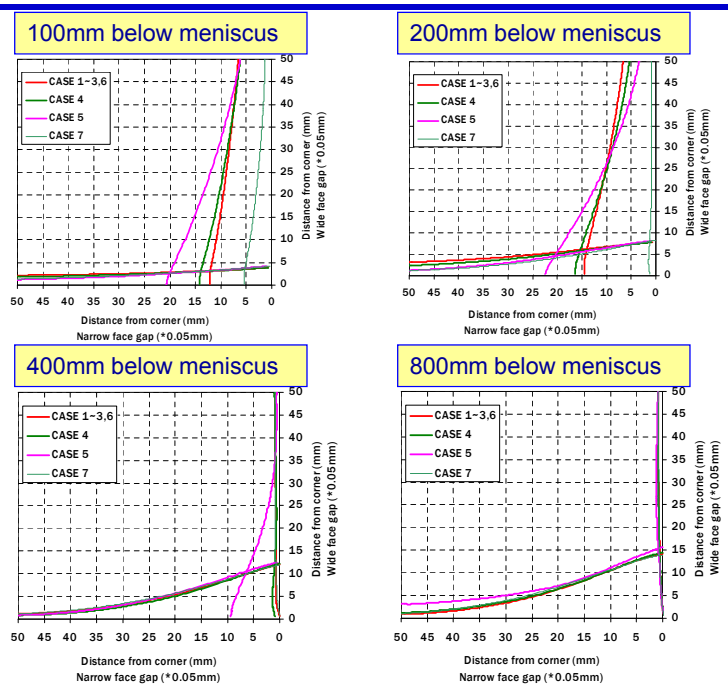

Figure 20. Analyzed Corner Gap profile

3.13. Calculation of Heat Flux at Off-Corner – Step 2

- Heat Flux equation across the Interfacial Gap

$$q_{\text{int}} = h_{gap}(T_s - T_{mold}) \quad \ldots (5)$$

$$h_{gap} = \frac{1}{\left(r_{contact} + \frac{d_{air}}{k_{air}} + \frac{d_{solid}}{k_{solid}}\right) + \left(\frac{1}{\frac{1}{\frac{d_{liquid}}{k_{liquid}} + \frac{d_{eff}}{k_{eff}}} + h_{rad}}\right)} \quad \ldots (6)$$

$$h_{rad} = \begin{cases} \dfrac{m^2\sigma\left(T_s^2 + T_{mold}^2\right)\left(T_s + T_{mold}\right)}{0.75a\left(d_{liquid} + d_{eff}\right) + \dfrac{1}{e_{mold}} + \dfrac{1}{e_{steel}} - 1} & \left(T_{mprime} \geq T_{cristal}\right) \\[2ex] \dfrac{m^2\sigma\left(T_s^2 + T_{cristal}^2\right)\left(T_s + T_{cristal}\right)}{0.75a\left(d_{liquid} + d_{eff}\right) + \dfrac{1}{e_{slug}} + \dfrac{1}{e_{steel}} - 1} & \left(T_{mprime} < T_{cristal}\right) \end{cases} \quad \ldots (7)$$

q_{int} = heat fluc transferred across gap (W/m^2)
h_{gap} = effective heat transfer coefficient across the gap (W/m^{2}K^1)
h_{rad} = radiation effective h (W/m^{2}K^1)
T_s = surface temperature of the steel shell (°C)
T_{mprime} = mold temperature + mold/slag contact resistance delta T (°C)
T_{mold} = surface temperature of the mold (°C)
T_{noliq} = surface temperature of the mold at no liquid layer (°C)
$T_{crystal}$ = mold flux crystallization temperature (°C)
$r_{contact}$ = flux/mold contact resistance (m^{2}K/W)
d_{air}, d_{solid}, d_{liquid}, d_{eff} = thickness of the air gap, solid, liquid flux and oscillation mark layers (mm)
k_{air}, k_{solid}, k_{liquid}, k_{eff} = conductivity of the air gap, solid, liquid flux and oscillation mark layers (W/mK)
m= flux refractive index
σ= Stefan Boltzman constant (W/m^{2}K^4)
a= flux absorption coefficient (m^{-1})
e_{steel}, e_{mold}, e_{slag} = steel, mold and slag emmisivities

If the oscillation marks are filled with liquid flux

$$k_{eff} = k_{liquid} \quad \ldots (8)$$

If the oscillation marks are filled with liquid flux and air

$$k_{eff} = \frac{\left(T_s - T_{cristal}\right)}{\left(T_{noliq} - T_{cristal}\right)} k_{liquid} + \frac{\left(T_{noliq} - T_s\right)}{\left(T_{noliq} - T_{cristal}\right)} k_{air} \quad \ldots (9)$$

3.13. Calculation of Heat Flux at Off-Corner – Step 2

- Assumption

Corner Gaps were filled with

CASE 1,4~7	CASE 2	CASE 3
Liquid Flux or Air	Liquid Flux	Air

Z <= 270 (Wide Face),320 (Narrow Face)

$$\begin{cases} d_{air} = d_{air-center} = 0 \\ d_{solid} = d_{sol-center} \\ d_{liquid} = d_{liq-center} + d_g \\ d_{eff} = d_{eff-center} \end{cases} \quad \ldots (10)$$

$$\begin{cases} d_{air} = d_{air-center} = 0 \\ d_{solid} = d_{sol-center} \\ d_{liquid} = d_{liq-center} + d_g \\ d_{eff} = d_{eff-center} \end{cases} \qquad \begin{cases} d_{air} = d_{air-center} + d_g = d_g \\ d_{solid} = d_{sol-center} \\ d_{liquid} = d_{liq-center} \\ d_{eff} = d_{eff-center} \end{cases} \quad \ldots (12)$$

Z > 270 (Wide Face),320 (Narrow Face)

$$\begin{cases} d_{air} = d_{air-center} + d_g = d_g \\ d_{solid} = d_{sol-center} \\ d_{liquid} = d_{liq-center} \\ d_{eff} = d_{eff-center} \end{cases} \quad \ldots (11)$$

d_{air}, d_{solid}, d_{liquid}, d_{eff} = thickness of the air gap, solid, liquid flux and oscillation mark layers (mm)

$d_{air-center}$, $d_{sol-center}$, $d_{liq-center}$, $d_{eff-center}$ = thickness of the air gap, solid, liquid flux and oscillation mark layers at the Center from CON1D result (mm)

d_g = Corner Gap (mm)

z= distance below meniscus (mm)

3.13. Calculation of Heat Flux at Off-Corner – Step 2

- Calculated Heat Flux ratio at the Corner

$$R_{corner} = q_{int-corner} / q_{int-center} \quad \ldots (13)$$

R_{corner} = heat flux ratio at the corner

$q_{int-corner}$ = heat flux at the corner (W/m^2)

$q_{int-center}$ = heat flux at the center (W/m^2)

Heat Flux ratio: Corner / Wide face center

200mm below meniscus | 400mm below meniscus

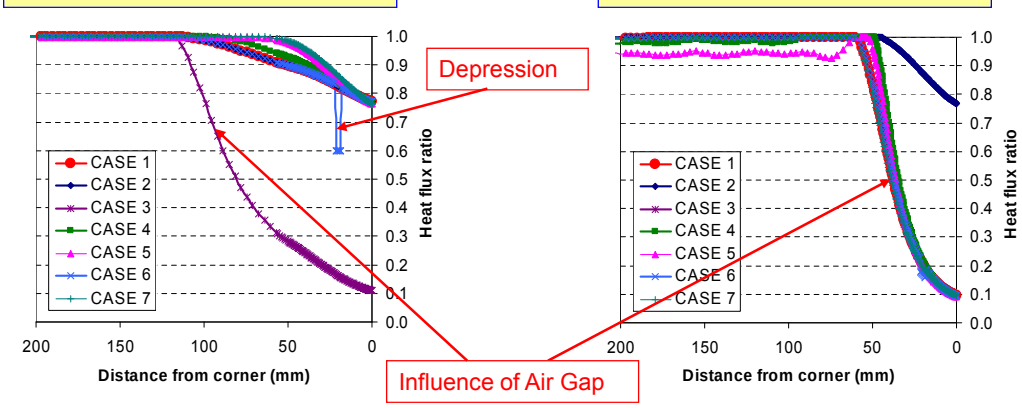

Figure 21. Calculated Wide Face Heat Flux at the Off-Corner

3.13. Calculation of Heat Flux at Off-Corner – Step 2

Heat Flux ratio: Corner / Wide face center

200mm below meniscus

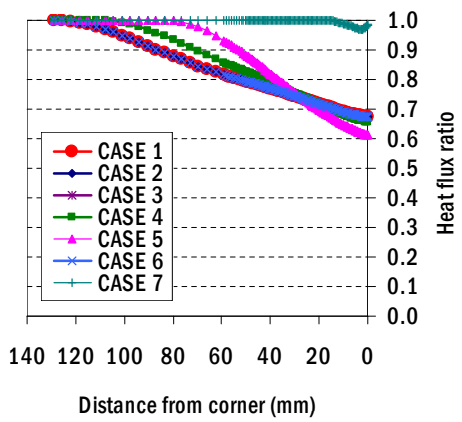

400mm below meniscus

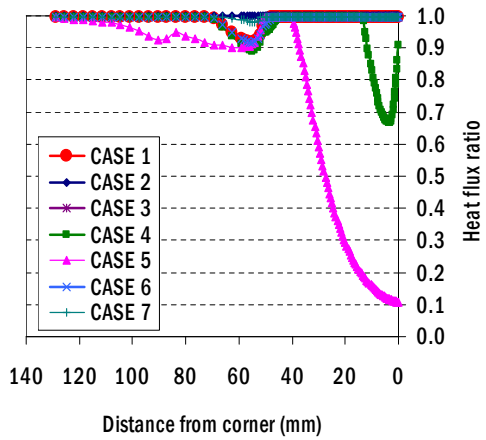

Figure 22. Calculated Narrow Face Heat Flux at the Off-Corner

3.14. Model Verification with Plant

Breakout Shell Thickness (Fs=35%)

Center

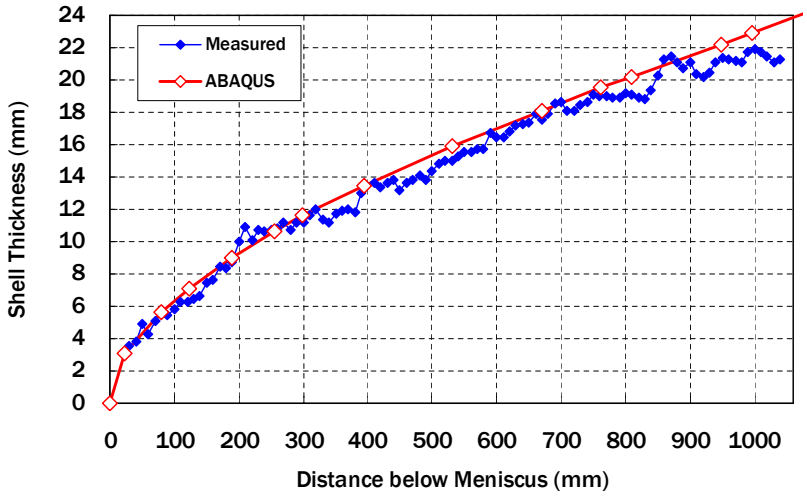

Figure 23. Comparison between ABAQUS calculated Shell Thickness profile and measurements from BO shell

3.14. Model Verification with Plant

Breakout Shell Thickness (Fs=35%)

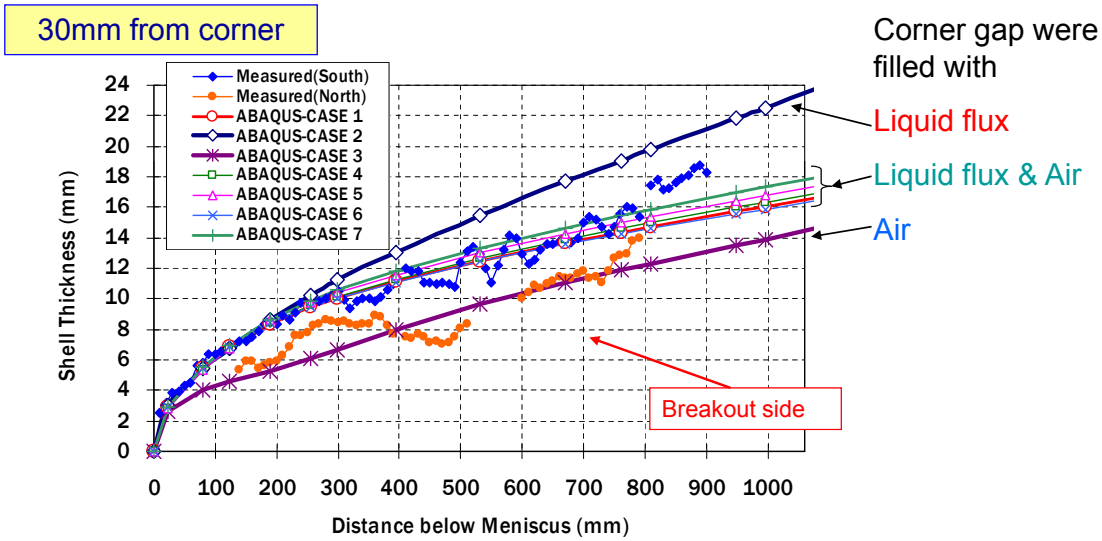

Figure 24. Comparison between ABAQUS calculated Shell Thickness profile and measurements from BO shell

3.14. Model Verification with Plant

Uniformity rate of the shell (Fs=100%)

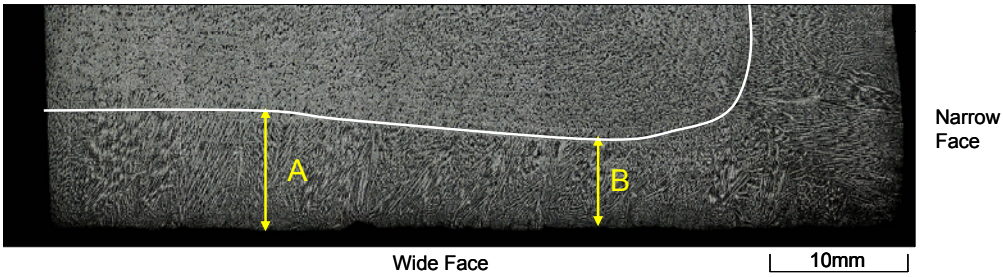

Microstructure at the Corner of the slab which is 5m before BO

Uniformity rate of the shell = B/A

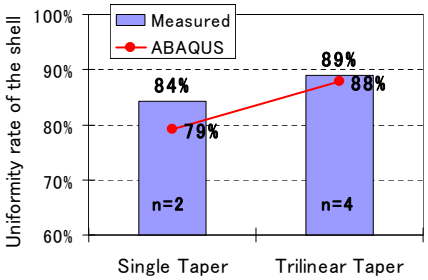

Figure 25. Comparison between ABAQUS calculated Solidification and measurements from White-Band

4. Evaluation of Hot-tearing Criteria
(ABAQUS Damage Strain / Nagata's Critical Strain)

- Critical hot tearing strain quantified by Nagata (Nippon Steel) :

$$\varepsilon_c = \varepsilon_{co}(\dot{\varepsilon}/3\times10^{-4})^{-0.167} \quad \ldots (14)$$

$$\varepsilon_{co} = 6.02\eta^{-2.13} \cdots\cdots 1 \le \eta \le 3$$
$$= 0.77\eta^{-0.258} \cdots\cdots 3 < \eta \quad \ldots (15)$$

- Brittle temperature zone (BTZ) width :

$$\eta = d(T_s) - d(ZDT) \quad \ldots (16)$$

d: distance from surface

- Average inelastic strain rate in BTZ :

$$\dot{\varepsilon} = \frac{\varepsilon(T_S) - \varepsilon(ZDT)}{t(T_S) - t(T_{ZDT})} \quad \ldots (17)$$

- Damage index :

$$D = \varepsilon_{dmg} / \varepsilon_c \quad \ldots (18)$$

$$\varepsilon_{dmg} = \varepsilon(ZDT) - \varepsilon(T_S) \quad \ldots (19)$$

Ts made from Fe-Me binary phase diagram

$$T_S = \theta_S - 20.5[\%Si] - 6.5[\%Mn]$$
$$-2.0[\%Cr] - 1.5[\%Ni] - 5.5[\%Al]$$
$$-156[\%P] - 700[\%S] \quad \ldots (20)$$

$$\theta_S = 1536 - 420[\%C] \cdots\cdots [\%C] \le 0.10$$
$$= 1494 \cdots\cdots 0.10 < [\%C] \le 0.185 \quad \ldots (21)$$
$$= 1525.2 - 168.8[\%C] \cdots\cdots 0.185 < [\%C]$$

ZDT made from ZDT mesured data

$$ZDT = T_S - \Delta T_C - \Delta T_{PS} \quad \ldots (22)$$

$$\Delta T_C = 92.86[\%C] - 18 \cdots\cdots [\%C] \le 0.14$$
$$= 700[\%C] - 103 \cdots\cdots 0.14 < [\%C] \le 0.18$$
$$= -466.7[\%C] + 107 \cdots\cdots 0.18 < [\%C] \le 0.24$$
$$= -5 \cdots\cdots 0.24 < [\%C] \le 0.50 \quad \ldots (23)$$

$$\Delta T_{PS} = 1007[\%P] + 1411[\%S] \quad \ldots (24)$$

Nagata et al., Tetsu- to- Hagane, 76;2(1990),pg. 214

4. Evaluation of Hot-tearing Criteria
Compare: effective shell thickness based on ZDT

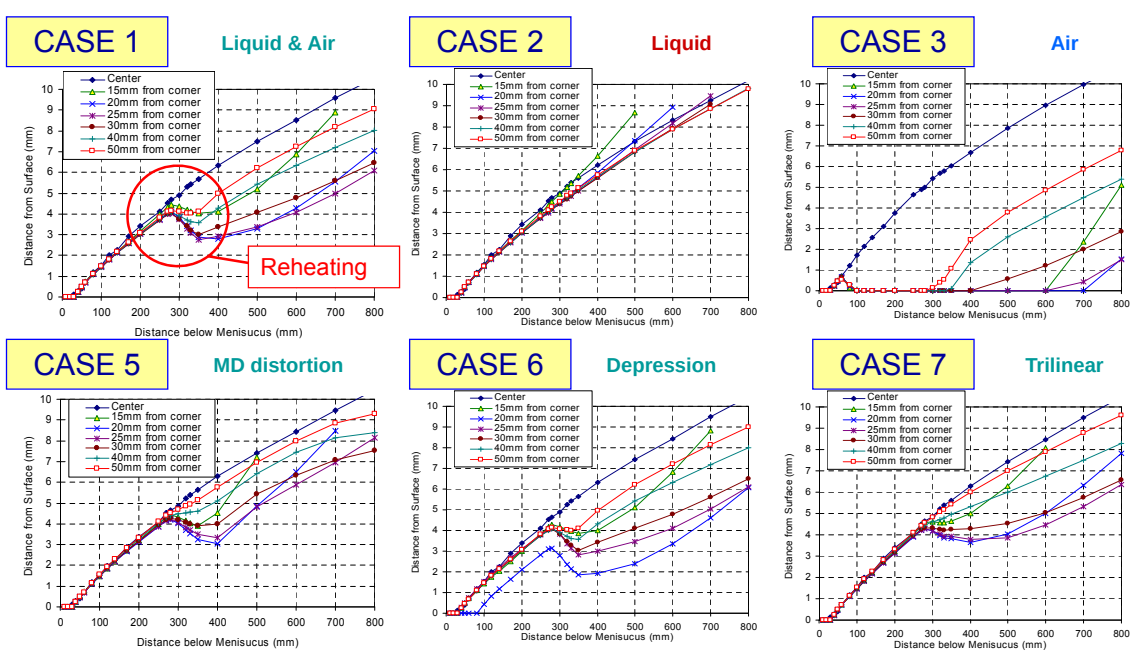

Figure 26. Analyzed Wide Face ZDT distance from surface

4. Evaluation of Hot-tearing Criteria

Compare computed Damage strain

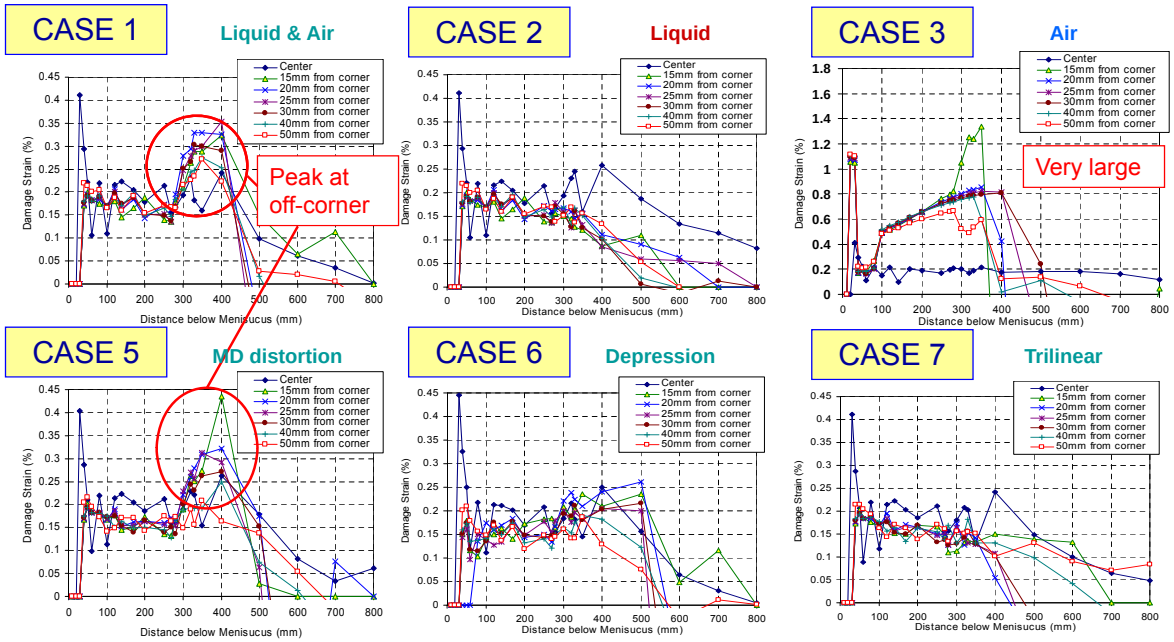

Figure 27. Analyzed Wide Damage Strain profile

4. Evaluation of Hot-tearing Criteria

Compare computed Inelastic strain

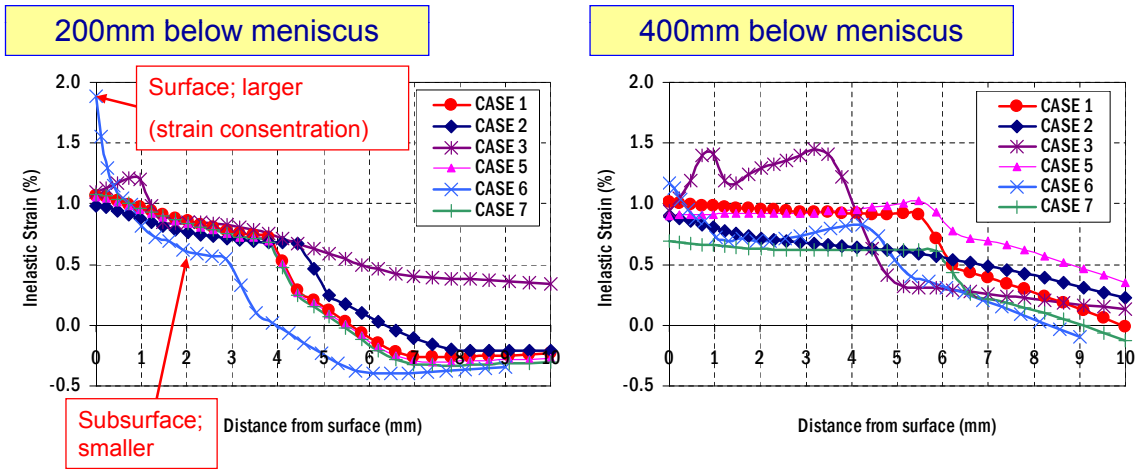

Figure 28. Analyzed Wide Face Inelastic Strain profile

4. Evaluation of Hot-tearing Criteria

Comparison of Nagata's Critical Strain

Wide face

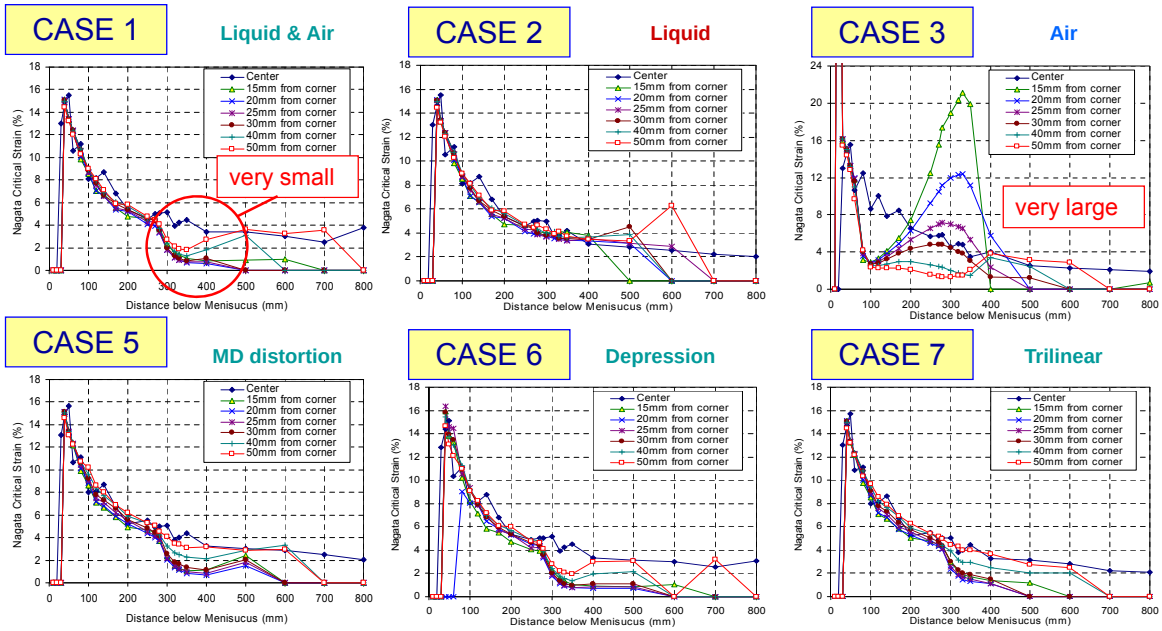

Figure 29. Analyzed Wide Face Critical strain profile

4. Evaluation of Hot-tearing Criteria

Comparison of Damage Index

Wide face

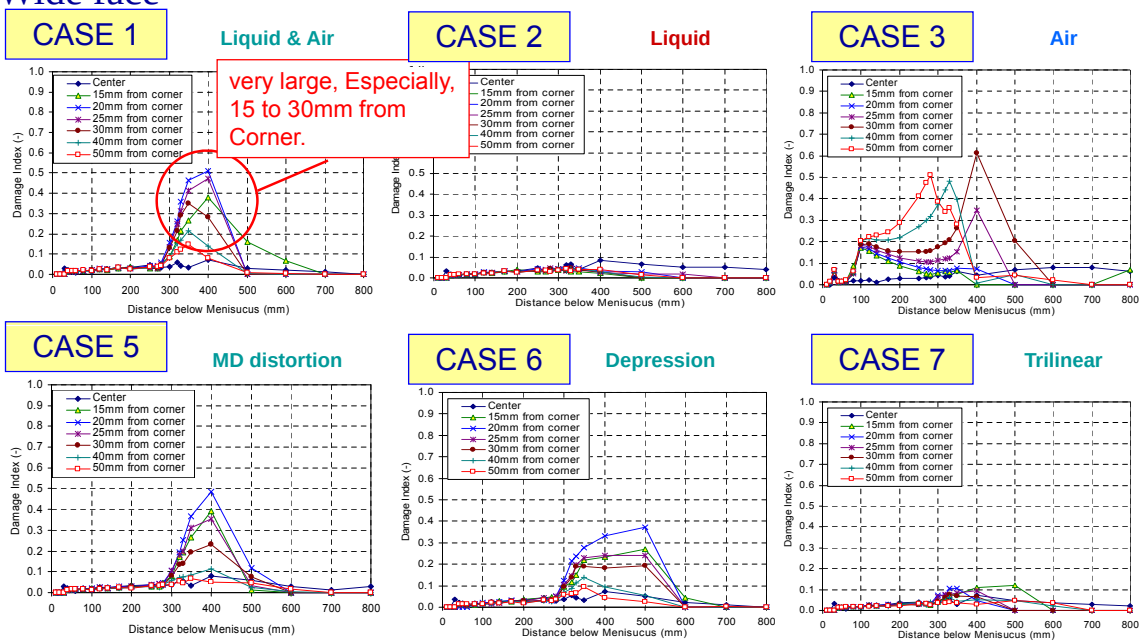

Figure 30. Analyzed Wide Damage index profile

4. Evaluation of Hot-tearing Criteria

Compare: Damage Index & Shell thickness at ZDT

Wide face (400mm below Meniscus)

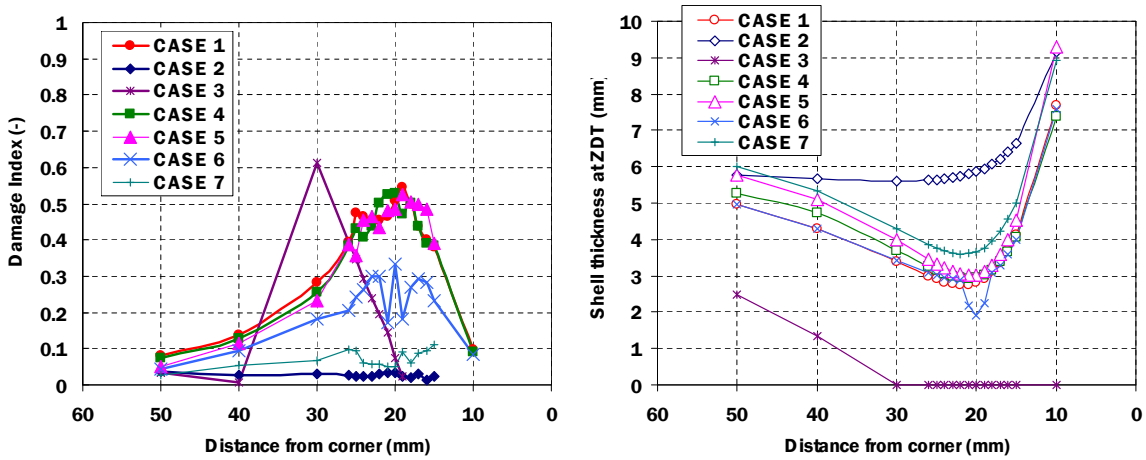

Figure 31. Damage index & Shell thickness profile along wide face

4. Subsurface Hot Tears

Evaluation by Nagata's Critical Strain

- Enlargement of Damage index was caused by following reasons.

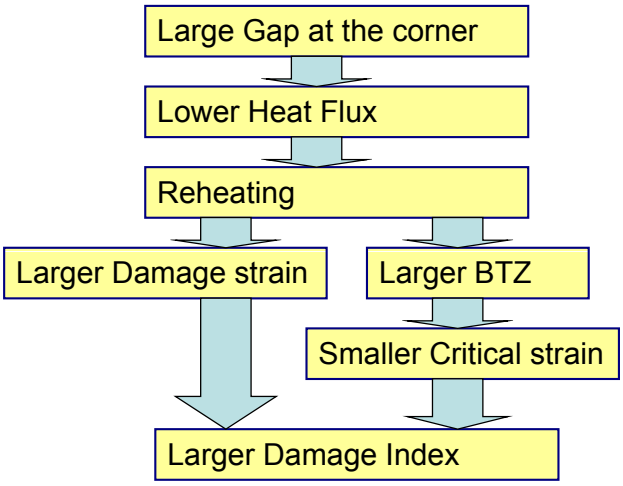

5. Conclusions

- Analyzed shell thickness with ABAQUS agreed well with the measured shell thickness from the breakout shell.
- Increase in Nagata's Critical Strain Damage index is caused by lower Heat Flux at the corner due to the calculated interfacial Gap.
- Corner gap filled with air causes larger increase in Damage Index than with liquid-flux gap.
- Mold distortion with rigid corner has little effect on Damage Index.
- Surprzingly: Depression decreases subsurface Damage Index due its ability to expand and contract. But, surface stress/strain at meniscus needs further work.
- Trilinear taper of narrow face helps to decrease Damage Index.
- The region of largest Damage index is almost the same as starting point of Breakout:
  20 - 30mm from the corner and 0 - 3mm from the surface.
- Calculated maximum Damage index is 0.61
- There must be some additional reason(s) to cause Breakout.